Developmental Biology 406 (2015) 222–234

Contents lists available at ScienceDirect

Developmental Biology

journal homepage: www.elsevier.com/locate/developmentalbiology

Wnt4 is essential to normal mammalian lung development

Arianna Caprioli [a,1], Alethia Villasenor [b,1], Lyndsay A Wylie [c,1], Caitlin Braitsch [d,1], Leilani Marty-Santos [d,1], David Barry [d], Courtney M. Karner [e], Stephen Fu [d], Stryder M. Meadows [f], Thomas J. Carroll [d], Ondine Cleaver [d,*]

[a] Dept. of Biology and Physical Sciences, Marymount Univ., 2807 N. Glebe Rd., Arlington, VA 22207, USA
[b] Developmental Genetics, Max Planck Institute for Heart and Lung Research, Germany
[c] Dept. of Genetics, Univ. of North Carolina, Chapel Hill, NC 27599, USA
[d] Dept. of Molecular Biology, Univ. of Texas Southwestern Medical Center, 5323 Harry Hines Blvd., Dallas, TX 75390, USA
[e] Dept. of Orthopaedic Surgery, Washington Univ. School of Medicine, St. Louis, MO 63131, USA
[f] Dept. of Cell and Molecular Biology, Tulane Univ., 2000 Percival Stern Hall, New Orleans, LA 70118, USA

ARTICLE INFO

Article history:
Received 10 October 2014
Received in revised form
31 July 2015
Accepted 26 August 2015
Available online 29 August 2015

Keywords:
Wnt4
Lung development
Fgf9
Wnt2
Fgf10
Ttf1
Trachea
Cell proliferation

ABSTRACT

Wnt signaling is essential to many events during organogenesis, including the development of the mammalian lung. The Wnt family member Wnt4 has been shown to be required for the development of kidney, gonads, thymus, mammary and pituitary glands. Here, we show that Wnt4 is critical for proper morphogenesis and growth of the respiratory system. Using *in situ* hybridization in mouse embryos, we identify a previously uncharacterized site of Wnt4 expression in the anterior trunk mesoderm. This expression domain initiates as early as E8.25 in the mesoderm abutting the tracheoesophageal endoderm, between the fusing dorsal aortae and the heart. Analysis of $Wnt4^{-/-}$ embryos reveals severe lung hypoplasia and tracheal abnormalities; however, aortic fusion and esophageal development are unaffected. We find decreased cell proliferation in $Wnt4^{-/-}$ lung buds, particularly in tip domains. In addition, we observe reduction of the important lung growth factors Fgf9, Fgf10, Sox9 and Wnt2 in the lung bud during early stages of organogenesis, as well as decreased tracheal expression of the progenitor factor Sox9. Together, these data reveal a previously unknown role for the secreted protein Wnt4 in respiratory system development.

1. Introduction

Wnt signaling is a critical regulator of embryonic development, tissue regeneration and homeostasis, in organisms ranging from Hydra to humans. Indeed, Wnts regulate the formation of many different organs and tissues, including the kidney, intestine, bone, skin, heart and lung, often relaying essential cell–cell communication between different tissue layers, such as epithelium and mesenchyme (Das et al., 2013; DasGupta and Fuchs, 1999; Grigoryan et al., 2008; Kim et al., 2005; Pinto et al., 2003). Wnts are also among the most influential group of signals that support stem cells within their niches, regulating self-renewal or differentiation status depending on context (Krausova and Korinek, 2014). Disruptions in Wnt signaling can lead to severe consequences for the developing embryo and to a number of pleiotropic human pathologies, including pulmonary fibrosis and cancer (Konigshoff and Eickelberg, 2010). However despite the fact that the Wnt signaling pathway has been heavily investigated in humans and model organisms, many questions as to how and where Wnt signals function remain open.

Since the identification of the first Wnt gene, Wnt1 (Nusse and Varmus, 1982; Thomas and Capecchi, 1990), 19 members have been discovered in mammals. Wnt proteins comprise a diverse group of glycoproteins that share a conserved wnt domain. This domain is characterized by the presence of 22–24 cysteine residues that act as a site of palmitoylation, which in turn allows for their secretion and interaction with Wnt receptors called Frizzleds (Fzd). Upon binding to a Fzd receptor and a LRP/Arrow family coreceptor, Wnts can activate multiple signaling cascades that can be divided into three different pathways: the “canonical” WNT/β-catenin pathway, and the non-canonical WNT/Ca^{++} and WNT/JNK pathways (Gordon and Nusse, 2006). The downstream effects of Wnt signaling include a wide range of cellular responses including cell fate determination, proliferation and differentiation. Together, these Wnt-regulated cellular processes have been shown to underlie morphogenetic events, including branching of the lung epithelium (Dean et al., 2005; Kadzik et al., 2014).

* Corresponding author. Fax: +1 214 648 1196.
E-mail address: ondine.cleaver@utsouthwestern.edu (O. Cleaver).
[1] Equal contributions.

http://dx.doi.org/10.1016/j.ydbio.2015.08.017
0012-1606/

Wnt genes are expressed in, and critical for, most developing organs. Wnt signaling in embryonic tissues can be readily observed using various reporters of Wnt activity. TOPGAL and BATGAL are two such mouse lines. Both TOPGAL and BATGAL contain a LEF/TCF inducible promoter driving the β-galactosidase gene and report canonical Wnt activity. Likewise, Axin2^{LacZ}, a stable knock-in of LacZ into the endogenous *axin* locus, is another reporter of canonical Wnt activity. All three of these reporters have been used to demonstrate that the lung is a site of canonical Wnt signaling (Al Alam et al., 2011). Indeed, multiple Wnts are expressed in embryonic lung tissues and are critical for lung development. Wnt7b, for instance, is detected in the lung epithelium as early as E9.5 and its loss results in lung hypoplasia (Shu et al., 2002). Wnt7b was shown to stimulate embryonic lung growth by coordinately increasing the replication of both epithelium and mesenchyme via different frizzled receptors (Rajagopal et al., 2008). Wnt5a regulates distal lung formation and its loss results in lung overgrowth, including expansion of the stromal interstitium (Li et al., 2002). Simultaneous loss of both Wnt2 and Wnt2b results in hypoplastic lungs (Goss et al., 2009b), indicating that Wnt2 and Wnt2b have functionally redundant roles in lung progenitor specification. It is therefore clear that coordination of multiple Wnts is required for proper development of the mammalian lung buds. However, the question remains as to whether additional unidentified Wnts further contribute to lung formation.

Wnt4 has long been known to regulate organ formation during embryogenesis. Notably, Wnt4 plays significant roles during kidney tubulogenesis and patterning (Naylor and Jones, 2009; Saulnier et al., 2002; Stark et al., 1994), sex determination (Kim et al., 2006), as well as the development of the adrenal gland (Heikkila et al., 2002), mammary gland (Brisken et al., 2000), pituitary gland (Treier et al., 1998), neuromuscular junction (Strochlic et al., 2012) and thymus (Heinonen et al., 2011). Wnt4 directs diverse molecular functions during the development of these organs. For instance, in the pituitary gland, Wnt4 is necessary for the expansion of ventral cells, while in the mammary gland, thymus, and the kidneys, Wnt4 controls mesenchymal-to-epithelial transition (MET) and epithelial cell proliferation. Whether Wnt4 plays analogous roles in additional organs, such as lung or other components of the respiratory system, has been heretofore unknown.

Here, we report a new role for Wnt4 during embryogenesis in lung bud outgrowth during embryogenesis. First, we identify a previously unrecognized domain of Wnt4 gene expression in the mesenchyme of the anterior trunk. This transient expression of Wnt4 gene transcription is sandwiched between the heart and the dorsal aortae during initial lung evagination from the foregut epithelium and early lung budding. Over developmental time, midline trunk Wnt4 expression declines and lung buds grow and extend beyond this domain of expression; therefore exposure of lung buds to Wnt4 is early and transient. We find that genetic ablation of Wnt4 during embryogenesis results in the early loss of Ttf1 and subsequent severe hypoplasia of lung buds, with a more significant reduction of the left lung. This phenotype had previously gone unrecognized as Wnt4$^{-/-}$ pups die shortly after birth, which was ascribed to failure of kidney development. We find that during lung outgrowth, Fgf9, Wnt2 and cell proliferation are all reduced in the absence of Wnt4. We also find that Wnt4$^{-/-}$ embryos exhibit abnormal tracheal ring formation, but no detectable defects in dorsal aortae fusion or esophagus formation. Together, these findings identify a novel role for Wnt4 in the anterior embryonic axis and place it, along with other known Wnts, as an important mediator of lung morphogenesis.

2. Materials and methods

2.1. Whole-mount in situ hybridization and RNA probes

Mice were maintained in a pathogen free facility following ARCRAC direction. After mating, females were checked every morning and plug was set as E0.5. At specific time points the pregnant females were sacrificed with CO_2 followed by cervical dislocation. Embryos were dissected out and isolated. Depending on the age of the embryos, the allantois (or the yolk sac) was used for genotyping. For embryos older than E11, the respiratory organs (trachea and lungs) were removed from the embryos and processed separately. Whole-mount *in situ* hybridization was carried out using digoxigenin-labeled probes and standard procedures previously described (Carroll et al., 2014). Full length *Wnt4, Wnt5a, Wnt7b, Wnt2/2b, Cx40, Ttf1, Fgf9, Fgf10, Shh, Sox9, Bmp4, EfnB2, Bmp7, FoxA1* mouse clones were obtained from Open Biosystems to generate RNA probes. Embryos were stained in whole mount and photographed, then embedded in paraffin and sectioned at 8 μm thickness. All experiments were carried out using $n \geq 3$ control or Wnt4$^{-/-}$ embryos (for Fgf9/10 probes embryos analyzed, 2 lung buds each-$n \geq 5$ control or Wnt4$^{-/-}$ embryos).

2.2. Whole-mount cartilage staining

Pregnant females were sacrificed to isolate E18.5 embryos, or newborns were separated from the mother at birth. Animals were then sacrificed as per IACUC indications. The respiratory system was dissected out and fixed in 99% ethanol overnight, then transferred to Acetone for 24 h. The respiratory system was stained with the method developed by Wallin et al., (1990) in a solution containing 1 volume 0.3% Alcian Blue, 1 volume of 0.1% Alizarin Red and 1 volume of Glacial Acetic Acid in 70% ethanol. A solution of 1% KOH was used for clearing the unstained tissue. Images were taken with a NeoLumar stereomicroscope (Zeiss) using a DP-70 camera (Olympus).

2.3. Antibody staining on sections

E11.5 trachea/esophagus trunk regions were dissected out and fixed in 4% PFA overnight at 4 °C and then embedded in paraffin and sectioned at 10 μm. Slides were deparaffinized with xylene, rehydrated, and then permeabilized with 0.1% Triton-X-100 in PBS (PBST) for 5 min at room temperature (RT). Slides were blocked for 1 h at RT with CAS-block (Invitrogen) and then incubated overnight with primary antibodies at 4 °C: 1:100 dilution of Sox9 (Millipore AB5535), 1:200 pHH3 (Millipore 06-570) and/or 1:100 E-cadherin (BD Transduction 610182) in CAS-block. The following day, slides were rinsed with PBST and then incubated in a 1:500 dilution of secondary antibody in CAS-block for 4 h at RT. Slides were rinsed with PBS and then mounted with Prolong Gold Antifade reagent with DAPI (Invitrogen) and imaged on a Zeiss 510 confocal. Quantification of pHH3^{+} cells on sectioned lung tissue was carried out using one way Anova with Turkey's correction (lungs analyzed, 2 lung buds each-Wnt4$^{+/+}$ $n=8$, Wnt4$^{+/-}$ $n=17$, and Wnt4$^{-/-}$ $n=9$).

2.4. Whole-mount TUNEL stain

Fixed tissues were rinsed with PBS and then incubated in equilibrium buffer (130 mM sodium cacodylate, 1 mM cobalt chloride and 30 mM Tris–HCl, pH7.2) for 1hr at RT with agitation. The tissue was incubated with reaction buffer (equilibrium buffer, 1:100 250 units rTdT, 1:100 1nmol biotinylated nucleotides [Roche]) overnight at RT. The next day tissues were washed in PBS at RT for 2 h, then overnight at 4 °C. The following day tissue was

incubated in streptavidin conjugated DyeLight-647 or -488 (Jackson Immuno Research, 1:200 in PBS) for 1 h or longer with agitation. After fluorescence was visible, tissue was washed thoroughly with PBS and then dehydrated in methanol. The tissue was then imaged in BABB solution.

2.5. Whole-mount pHH3 stain

Fixed tissues were washed with PBS, permeabilized with PBS/1% Triton-X-100 for 1 h, then blocked in CAS-block (Invitrogen) for 2 h at RT. The block was replaced with anti-phospho-Histone-H3 antibody (Ser10) (Millipore 06-570) dissolved in CAS-block (1:100) and incubated overnight at 4 °C with agitation. The next day the tissues were washed with PBST (0.1% Tween20/PBS) then the secondary goat anti-rabbit antibody (Invitrogen A11034) diluted in CAS-block was added to the tissue and incubated for 2 h at room temperature. Lastly, the tissues were washed in PBS and imaged. Quantification and statistical analyzes (for pHH3 proliferation/TUNEL stainings) were performed after analyzing 5 representative fields of view (from different sections) through nascent lung buds using ImageJ (embryos analyzed, 2 lung buds each-Wnt4$^{+/+}$ $n=15$, Wnt4$^{+/-}$ $n=25$, and Wnt4$^{-/-}$ $n=19$).

2.6. Whole-mount immunohistochemistry (DAB) staining

Embryos at E8.25-E9.0 were fixed in 4:1 Methanol:DMSO at 4 °C overnight, treated with 4:1:1 MetOH:DMSO:H_2O_2 for 10 h at 4 °C and stored in 100% MetOH at −20 °C. For staining, embryos were re-hydrated in PBS; blocked in PBSMT (PBS, 2% Carnation skim milk, 0.5% Triton X-100) for 2 h; and incubated with primary antibody overnight (1:200 PECAM, BD Biosciences 553370). Samples were washed 6 times with PBSMT for 6 h and incubated with secondary antibody at 4 °C (1:200 anti-rat HRP, Santa Cruz). The next day, embryos were washed with PBST for 10 hrs. For developing, samples were incubated for 30 min in ABC solution (Vector labs PK-6200), washed, and developed with Diaminobenzidine (DAB). Finally, for visualization samples were cleared in BABB (1:2 Benzyl alcohol:Benzyl benzoate) after MetOH dehydration.

2.7. Hematoxylin eosin (H&E) staining

Sections were deparaffinized in xylene for 10 min, followed by ethanol washes from 100% to 70%, then submerged in Harris' Hematoxylin solution for 30 s, rinsed in water, de-stained in 0.5% acid alcohol, rinsed in water, submerged in 1% alcoholic Eosin for 30 s, taken through ethanol wash series from 50% to 100%, xylene series for 5 min each, then coverslipped with Permount (Fisher) and dried.

2.8. RNA isolation and real-time quantitative RT-PCR

Total RNA (250 ng) from mouse E11.5 lung and E13.5 trachea (isolated using RNeasy Micro Kit, Qiagen) was used to generate cDNA from each lung or trachea using SuperScript II (Invitrogen). 1 µl cDNA in Power SybrGreen Master Mix (Applied Biosystems) was used for real-time quantitative reverse transcriptase polymerase chain reaction (qPCR) analysis (CFX96, Bio-Rad) of gene expression using *Fgf10* primers: 5′-GAT TGA GAA GAA CGG CAA GG-3′ and 5′- GTT GCT GTT GAT GGC TTT GA-3′. Primers for *Fgf9*, *Wnt2*, *Sox9*, *Cyclophilin*, and *HPRT* have been previously described (Al Alam et al., 2011; DasGupta and Fuchs, 1999; Grigoryan et al., 2008; Pinto et al., 2003; Segre et al., 1999). Gene expression levels were determined by PCR reactions (95 °C, 30 s; 60 °C, 30 s; 72 °C, 30 s; 35 cycles) (*Fgf9*, *Fgf10*, *Sox9*) or (95 °C, 30 s; 60 °C, 30 s; 72 °C, 30 s; 35 cycles) (*Wnt2*), and fluorescence was measured at 72 °C. Gene expression levels were calibrated based on the threshold cycle [C(t)] calibrated to a standard curve generated for each assay using a five-step 1:10 dilution curve of wildtype mouse E14.5 lung cDNA. Gene expression levels were normalized to *Cyclophilin* or *HPRT*. Data were collected from individual Wnt4$^{-/-}$ embryos ($n=4$) and littermate controls (wildtype or Wnt4$^{+/-}$ $n=5$–8) and samples were analyzed in triplicate.

2.9. Statistical analysis

Statistical significance was determined by Student's *t*-test with $P < \leq 0.01$ or $P \leq 0.05$ as indicated. Data are reported as mean with standard error of the mean (s.e.m.). All experiments were carried out using $n \geq 3$ control or Wnt4$^{-/-}$ embryos.

3. Results

3.1. Wnt4 expression flanks tracheoesophageal groove and fusing aortae

To assess Wnt4 expression during early embryogenesis, we performed *in situ* hybridization on wildtype mouse embryos during onset of organogenesis (embryonic days E8.75 − 10.5). In addition to known domains of expression in the neural tube, reproductive tract and developing kidney (Stark et al., 1994; Vainio et al., 1999), we identified a previously unreported site of Wnt4 expression in a distinct patch along the anteroposterior axis, surrounding a portion of the anterior foregut (red arrows in Fig. 1A–C). Wnt4 expression initiated in this region as early as E8.25, appearing in two domains of the splanchnic lateral plate mesoderm, along the dorsal aspect of the open gut tube, at the level of the heart and anterior the intestinal portal (Fig. S1A). When compared to other Wnts expressed in this region, we found Wnt4 expression initiation in a pattern similar to Wnt2b, but preceded that of Wnt7b and Wnt5a (Fig. S1E–P′). Interestingly, expression of Wnt4 consistently initiated slightly earlier on the right side than on the left at E8.25 (Fig. S2A,B), however it appeared relatively equivalent on both sides by E8.75 and thereafter (Fig. S2C). Between E8.75 and E9.5, following embryonic turning, Wnt4 expression increased and was evident in the mesoderm associated with the foregut endoderm (Fig. 1A′), dorsal to the heart and ventral to the paired dorsal aortae, located between somites 1 and 3 (Fig. 1B′). By E10.5, this expression domain expanded posteriorly, reaching the upper limit of the forelimb bud (Fig. 1C, see also Fig. S1B–D).

To clearly define Wnt4 expression boundaries, we surgically removed the neural tube from whole mount stained embryos to reveal both internal staining and embryonic structures (Fig. 1A′–C′, D–I). At E8.25-8.75, Wnt4 was expressed in the foregut at high levels in two distinct domains, each lateral to the gut tube (Fig. 1A′). At this point during embryogenesis, few identifiable developing organs or tissues are present in this region of the trunk (Kaufman, 1992). Previous studies indicate that this region gives rise to the future tracheo-esophageal-lung primordia, and contains the anterior portion of the fusion point of the dorsal aortae (Morrisey and Hogan, 2010; and data not shown). By E10.5, Wnt4 expression domains fuse at the midline and expande both anteriorly and posteriorly, surrounding the future pharynx, tracheal/esophageal tubes and anterior stomach (Fig. 1C′).

To assess which developing structures might be subject to Wnt4 signaling in the foregut, we first compared Wnt4 expression with the arterial marker Connexin 40, Cx40 (Fig. 1D–F; Chong et al., 2011). Cx40 marks the dorsal aortae, the initial vessels that transport blood from the heart to early mouse embryo. The two aortae initiate as parallel vessels on each side of the notochord, running along the gut endoderm (Chong et al., 2011), and by E9.0 start to fuse along the length of the embryonic axis (data not

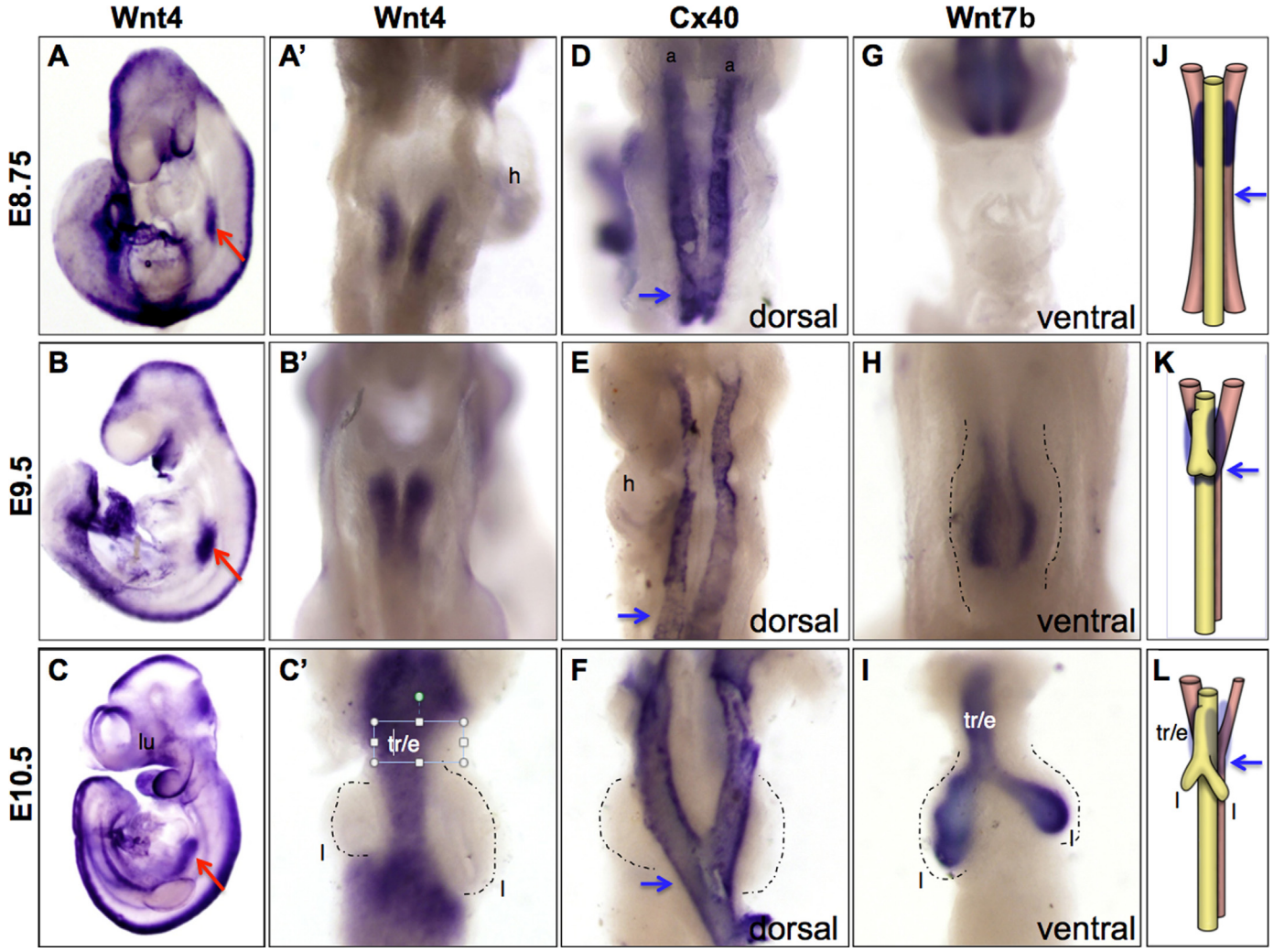

Fig. 1. Wnt4 expression in the mesenchyme near the developing dorsal aorta trachea, esophagus and lung. *In situ* hybridization of Wnt4 (A)–(C), lateral view and (A′)–(C′), dorsal view after removal of neural tube and aortae), Cx40 (D–F) and Wnt7b (G)–(I) at different developmental stages. E8.75 (A), (A′), (D), (G), and (J), E9.5 (B), (B′), (E), (H), (K), and E10.5 (C), (C′), (F), (I), and (L). (J)–(L) Schematic of Wnt4 trunk expression (purple) relative to the aortae (red tubes), esophagus and forming trachea/lung buds (yellow). (C′), (F), (H), (I) Lung buds are outlined with dotted line. Anterior point of aortae fusion (blue arrow). a, aorta; e, esophagus; h, heart; l, lungbud; tr, trachea.

shown), forming a single large vessel. The anterior boundary of fusion is located at the level of the second somite (data not shown), and anterior to this region the two aortae remain unfused, thus forming a "Y-like" structure. Interestingly, Wnt4 expression spans the aortic fusion point (compare Fig. 1A′ and D, and Fig. 1B′ and E). By E10.5, the aortae have fused completely along most of the length of the embryonic axis, and Wnt4 expression broadly overlapped the fusion point, both anteriorly and posteriorly (Fig. 1C′ and F) suggesting Wnt4 function in the fusion process.

Because the early trunk Wnt4 domain appeared to correlate with the presumptive lung field, we compared Wnt4 with the lung epithelial marker Wnt7b (Rajagopal et al., 2008) (Fig. S1 I–L). Indeed, Wnt4 was expressed in close proximity to the forming lungs and preceded Wnt7b expression by approximately 0.25 days (compare Fig. 1A′–C′, G–I). Initially, between E8.75 and E9.5, Wnt4 expression flanked the budding lung region (Fig. 1A, A′, B and B′, compare to budding lung marker Wnt7b,Fig. 1H), eventually expanding around the trachea, but becoming restricted from the growing distal lung tips (Fig. 1 compared to 1I). In addition, Wnt4 expression overlapped that of other Wnts (e.g. Wnt5a and Wnt2) in the vicinity of the developing lung (Fig. S1E–H, M–P). After E10.5, Wnt4 expression in the trunk faded, and by E14.5 expression was largely undetectable (data not shown). Thus Wnt4 expression flanked the lung territory only early during its development. Together, these data indicate that Wnt4 is transiently expressed in the region that contains the fusing dorsal aortae, the esophagus, the trachea and the lung buds (Fig. 1J–L). We next investigated the relationship between Wnt4 and structures arising in this territory.

3.2. *Initiation of Wnt4 expression is correlated with lung specification*

In order to further define which tissues expressed Wnt4 in the anterior trunk, we examined sections of embryos stained for Wnt4 transcripts. We found that Wnt4 expression initiated in a restricted domain of the lateral plate mesoderm, specifically the splanchnic mesoderm. The first two patches of Wnt4 expression appeared dorsal to the AIP, along the foregut endoderm, but at some distance ventral to the parallel dorsal aortae starting around E8.25 (Fig. 2A1–D1). As shown in schematics (Figs. 2B1–5) and embryonic sections (Fig. 2C–E), Wnt4 expression initiated in the trunk at the level of the heart around E8.25 (Figs. 2A1,2) as paired domains approximately two to three somites in length. These remained unpaired past E8.75 when the embryo turns (Fig. 2A2 and B2). By E9.0, the paired dorsal aortae come into proximity of one

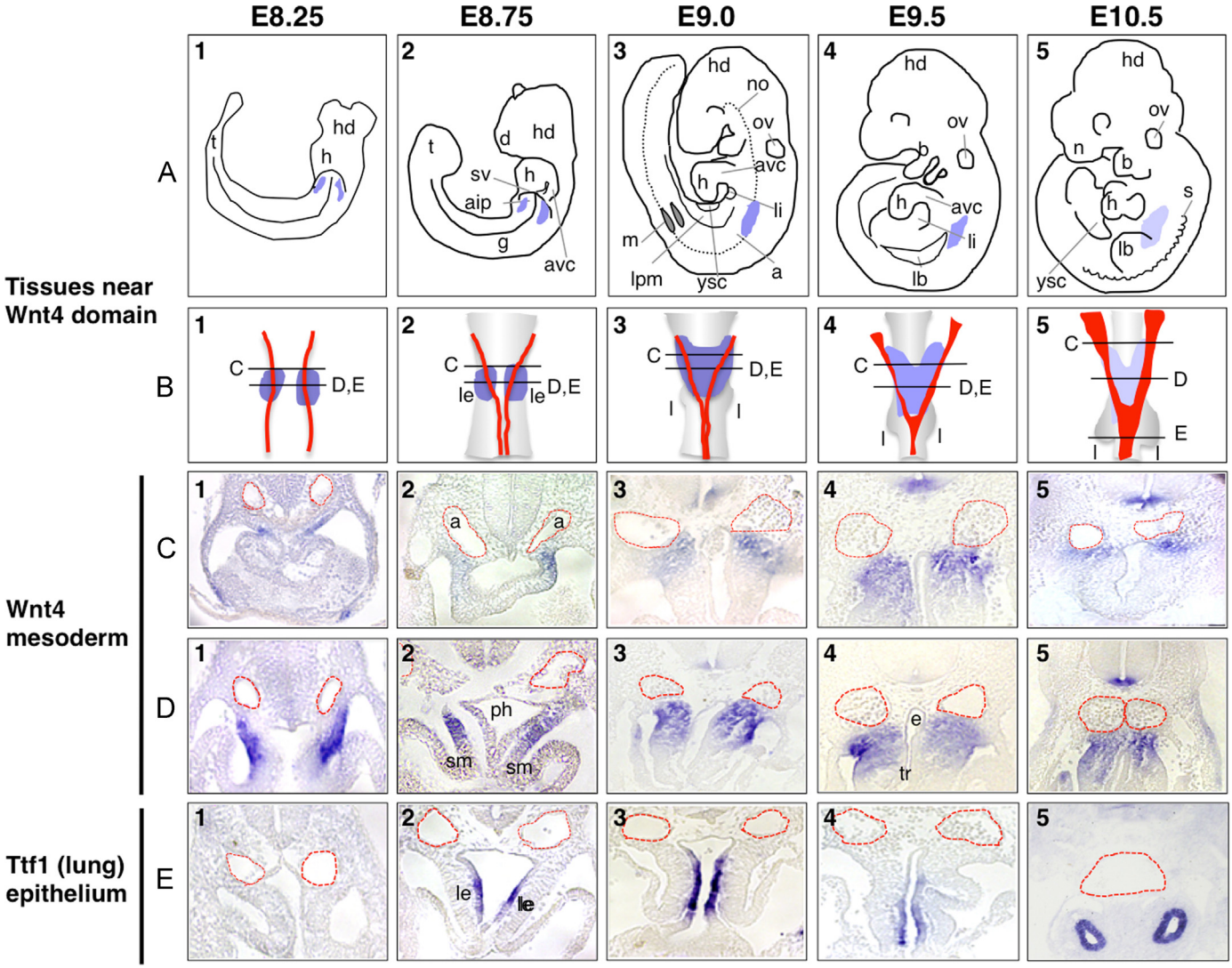

Fig. 2. Wnt4 is expressed in the mesoderm, around the aortic fusion point, trachea, esophagus and lung. (A1-5) Schematic showing lateral view of Wnt4 expression (purple) in the developing embryo relative to other structures. (B1-5) Schematic showing ventral view of Wnt4 expression (purple) during the aortic fusion (dorsal aortae, red) and lines depict the plane of sections in C, D, and E. (C)–(D) Transverse sections of Wnt4 at indicated stages. Aortae outlined by dotted red line. (C) and (D) or Ttf1 (E) *in situ* hybridization, dorsal is up and ventral is down. a, aorta; aip, anterior intestinal portal; avc, anterior vena cava; b, branchial arches; d, dicenphalon; e, esophagus; h, heart; hd, head; g, gut; l, lung bud; lb, limb bud; le, lung endoderm; li, liver; m, mesonephros; n, nose; no, notochord; ph, pharynx; t, tail; tr, trachea; ov, otic vesicle; s, somites; sm, splanchnic mesoderm; sv, sinus venosus; ysc, yolk sac.

another and fuse along most of the trunk axis, from the level of the second somite to the last somite in the tail. Wnt4 expression spanned from somite 2–3 to just anterior to the aortic fusion point (Figs. 2A3–4, B3-4, C3-4, D3–4 and data not shown).

Notably, prior to lung budding, Wnt4 expression directly abutted the pre-lung territory within the underlying epithelium, which expresses Ttf1 expression (two bilateral patches) (Fig. 2D–E). Indeed, we found that the region of expression of Wnt4 and Ttf1 overlapped early during development, but later became distinct. At E8.25, the developing gut has not yet folded into a tube, and Ttf1 expression in the pre-respiratory epithelium was not detectable (Fig. 2E1). Wnt4 expression, however, was observed in the mesoderm that overlays this domain (Fig. 2D1). Around E8.75, following embryonic turning, Ttf1 expression was found in the ventral endodermal epithelium of the anterior trunk. At this time, mesodermal Wnt4 was immediately juxtaposed to Ttf1-expressing endodermal epithelium (Figs. 2D2and2E2). This colocalization of expression domains continued through E9.0 (Figs. 2D3and2E3). However, Ttf1 expression localized more ventrally by E9.5, the time when the tracheal-esophageal groove forms and lungs begin to bud (Fig. 2E4). By contrast, the Wnt4 domain at this stage remained in the mesoderm around the esophageal endoderm, more dorsally (Fig. 2D4). By E10.5, Wnt4 expression remained immediately ventral to the two aortae, along the dorsal aspect of the gut tube, while the presumptive lung buds have emerged and grown ventro-laterally (Figs. 2D5and2E5). At this stage, Wnt4 expression remained adjacent to the endoderm that gives rise to the trachea and the esophagus (Kaufman, 1992). Given its observed expression domains, Wnt4 might regulate fusion of the anterior dorsal aortae and/or the morphogenesis or growth of the trachea, esophagus or lungs.

3.3. *Wnt4 is not required for patterning or positioning of the anterior aortic split*

Wnt4 is expressed in the mesenchymal compartment of the developing kidney and Wnt4 null embryos fail to develop kidneys (Stark et al., 1994). Wnt4 is thus a critical regulator of organogenesis,

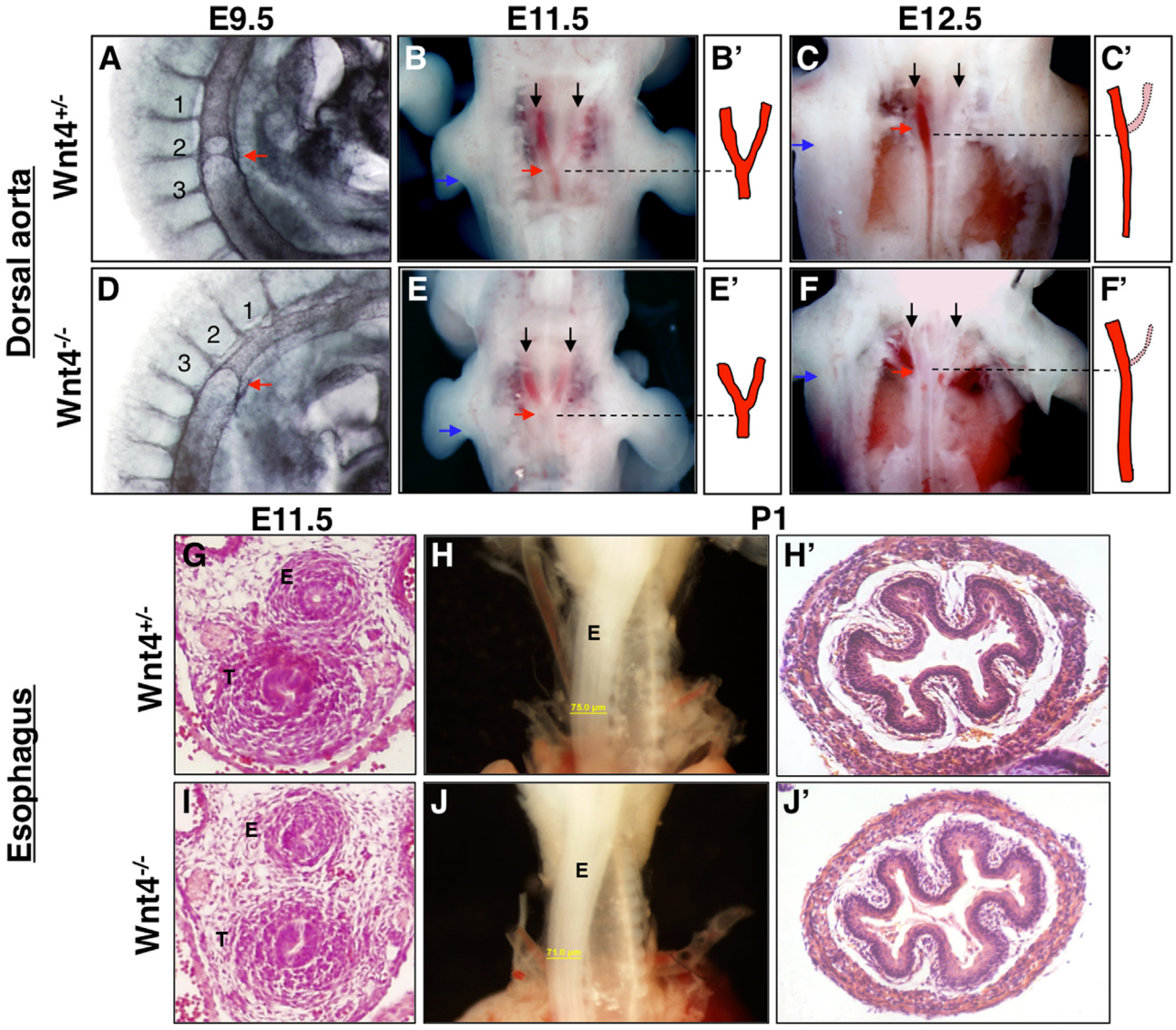

Fig. 3. Wnt4 is not required for aortae fusion or development of the esophagus. (A) and (D) Whole mount PECAM staining showing aorta fusion (red arrow). Numbers 1, 2, and 3 indicate somites pair number. (B), (C), (E), and (F) Dorsal view of whole dissected embryos show dorsal aortae (arrows) and location of aortae fusion point, relative to limb buds (dotted line). (B′), (C′), (E′), and (F′) Schematic depicting aortic fusion and regression shown in (B), (C), (E) and (F). (G)–(J′) Analysis of esophageal development by H&E staining (G), (H), (I′) and (J′) and whole mount imaging (H) and (J) in Wnt4$^{+/-}$ (G), (H) and (H′) and Wnt4$^{-/-}$ (I), (J) and (J′) embryos at E11.5 (G) and (I) and P0 (H), (H′), (J), (J′). E, Esophagus; T, Trachea.

so we reasoned that other organs and tissues in the vicinity of Wnt4 might exhibit defects in its absence. We therefore analyzed formation of multiple organs in the trunk of Wnt4 nulls and found that many organs were impaired in the absence of Wnt4. In addition to kidney agenesis (Stark et al., 1994), we found unexpected defects in the stomach, spleen and heart (Fig. S3), with pleiotropic defects including reduction in overall size.

To assess whether Wnt4 played a role during dorsal aorta development, we examined aortic fusion in E9.5 to E12.5 embryos. Whole mount staining for PECAM was used to observe the aortic fusion point in heterozygous embryos compared to Wnt4$^{-/-}$ littermates. In both wildtype and Wnt4$^{-/-}$ animals, the two aortae initiated fusion normally around E9.0 throughout most of the embryonic posterior trunk (data not shown). By E9.5, a single aorta can be observed in both sets of embryos, running from the level of the limb buds down to the tail (Fig. 3A). At the rostral end, the fusing aortae form a “Y” around somite 2 (this also happens in the tail, data not shown). By E11.5, the aortic bifurcation lies even with the posterior aspect of the forelimb (blue arrow Fig. 3B) in both wildtype and Wnt4$^{-/-}$ animals (we note that wildtype Wnt4$^{+/+}$ and heterozygous Wnt4$^{+/-}$ embryos displayed no defects in any organ, at any stage examined, and Wnt4$^{+/-}$ animals were viable and fertile—consequently, we use Wnt4$^{+/-}$ and Wnt4$^{+/-}$ interchangeably as controls throughout our studies). Anterior to the point of rostral fusion, the two aortae remained separated, but by E11.5 the right aortic branch (right alpha segment) started to regress by apoptosis (Molin et al., 2002). By E12.5, it was difficult to distinguish (right arrow Fig. 3C) and was largely gone by E13.5 (data not shown) (Moore and Persaud, 1993). At all stages examined, the aortic fusion point in Wnt4 mutants was located at the same antero-posterior level as heterozygous embryos (compare Fig. 3A and D; at E11.5–12.5 compare blue and red arrows in Fig. 3B, B′–E, E′ and C, C′–F, F′). There were no delays nor defects in aortic fusion observed, and no abnormalities in endothelial integrity or patterning (data not shown), suggesting Wnt4 is not required for dorsal aorta development.

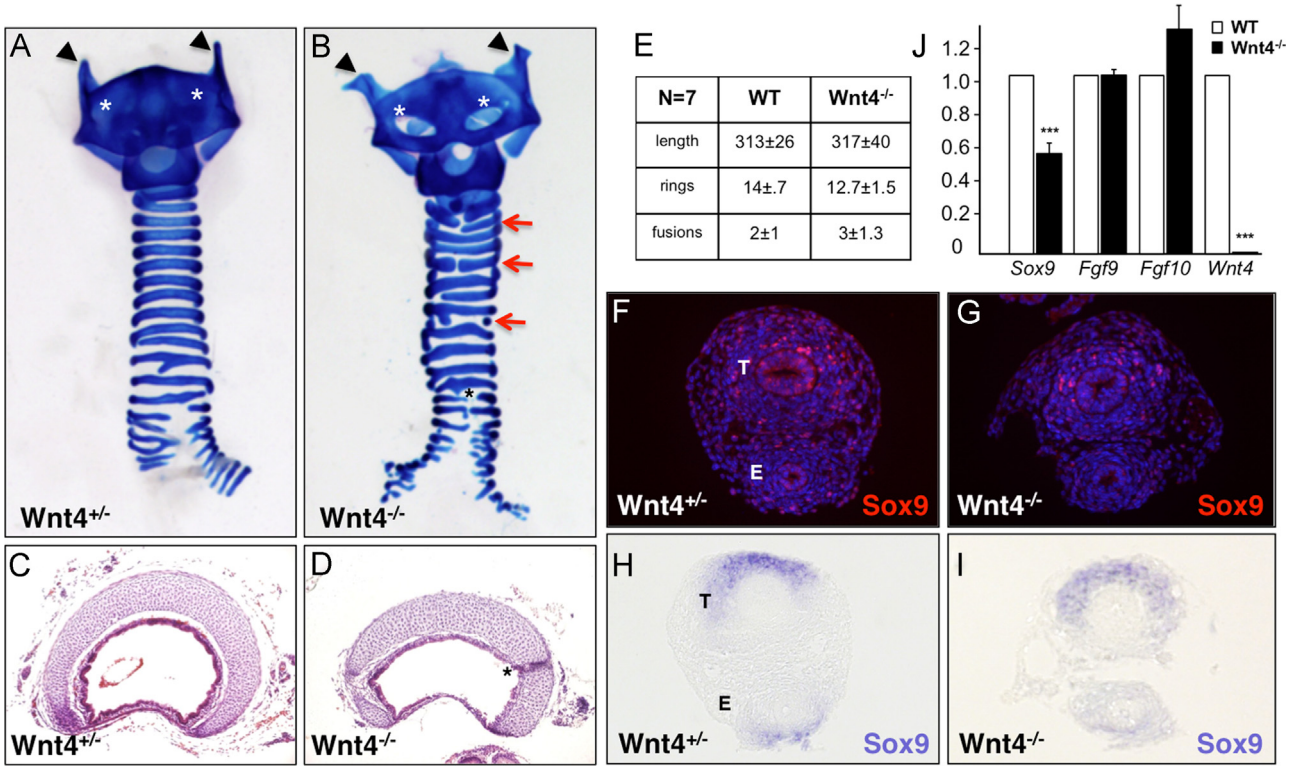

Fig. 4. Wnt4 is required for tracheal development. (A) and (B) Alcian blue staining of E18.5 tracheas from Wnt4$^{+/-}$ (A) and Wnt4$^{-/-}$ (B) animals. Red arrows denote ring malformations; arrowheads denote defective thyroid cartilage superior horns; white asterisks denote aberrantly open areas in the thyroid lamina; black asterisk indicates unfused cartilage rings. (C) and (D) Transverse sections of E18.5 tracheas stained with H&E. (E) Quantification of tracheal structures in Wnt4$^{+/-}$ and Wnt4$^{-/-}$ embryos at E18.5 ($n=7$). (F)–(I) Sox9 immunofluorescence (F) and (G) or *in situ* hybridization (H) and (I) on transverse sections of E11.5 trachea/esophagus and associated mesoderm from Wnt4$^{+/-}$ (F) and (H) and Wnt4$^{-/-}$ (G) and (I) tissues. (J) Quantification of Sox9 expression by qPCR analysis of E13.5 tracheas from WT and Wnt4$^{-/-}$ embryos. Data are shown as mean ± SEM; ***$p < 0.001$. E, Esophagus; T, Trache.

3.4. *The embryonic esophagus develops normally in the absence of Wnt4*

Given that Wnt4 expressing mesoderm also partly surrounded the developing esophagus, we examined whether the formation of this tissue occurred normally in Wnt4$^{-/-}$ mutants. Indeed, both Wnt4$^{-/-}$ embryos and newborn pups exhibited no apparent esophagus defects compared to that of their heterozygous counterparts (Fig. 3G–J). Esophagus in Wnt4$^{+/-}$ and Wnt4$^{-/-}$ embryos exhibited similar lumen diameters, epithelial integrity and stromal/smooth muscle coverage (Fig. 3G–J′ and data not shown).

3.5. *Patterning of tracheal cartilage rings requires Wnt4*

We next examined tracheal development in the absence of Wnt4. Wnt4$^{+/-}$ and Wnt4$^{-/-}$ tracheas were isolated from P0 pups shortly after birth and examined using Alcian blue staining to visualize cartilage and assess their length, number of rings and cartilage ring defects/fusions. Some Wnt4$^{-/-}$ pups displayed incomplete cartilage rings compared to their wildtype littermates (compare Figs. 4A and4B**).** Analysis of trachea sections showed that mutant rings were smaller and revealed more partial fusion events (black asterisk) visible via whole mount cartilage staining (compare Fig.4C and D). Cartilage rings of the bronchi were also smaller in the mutant as compared to heterozygotes. (We note that these tracheal defects were observed in approximately 1/3 of all Wnt4$^{-/-}$ P0 pups). Further observation of this portion of the respiratory tract also revealed mild abnormalities in the structure of the thyroid cartilage. The superior horns (arrowheads) in the heterozygous newborns are aligned with the thyroid lamina, while Wnt4$^{-/-}$ mice were often enlarged (5 out of 7) or misplaced (1 out of 7). Furthermore, the thyroid lamina (asterisk) of the transgenic homozygous mice was often incomplete, showing two sizable symmetric holes (Fig. 4A, B, white asterisks).

These observations reveal a role for Wnt4 in trachea formation. To characterize how absence of Wnt4 expression might impact tracheal cartilage ring formation, we examined whether the expression of the chondrogenic progenitor marker Sox9 was affected prior to tracheal ring formation (Fig. 4F–I). We found that at E11.5, the presumptive tracheal territory of Wnt4$^{+/-}$ embryos displayed both epithelial and mesenchymal Sox9 expression, which was reduced in Wnt4 nulls at the protein (Fig. 4F–G) and the transcript levels (Fig. 4H–I**).** To further confirm this observation, we isolated tracheas from Wnt4$^{+/-}$ and Wnt4$^{-/-}$ embryos and carried out quantitative PCR (pPCR) to assess Sox9 and Wnt4 expression (Fig. 4J), confirming down-regulation of Sox9 in the absence of Wnt4 at this stage.

3.6. *Wnt4 is essential to normal lung budding and growth*

Because Wnt4 expression was also adjacent to the lung anlagen, we investigated whether Wnt4 might play a role during lung development. Wnt4$^{+/-}$ and Wnt4$^{-/-}$ lung buds were isolated at various embryonic stages and analyzed. To visualize lung epithelium, *in situ* hybridization was carried out with the lung epithelial marker Wnt7b. At E10.5, when the lung epithelium has already budded, we observed that the Wnt4$^{-/-}$ left lung bud was slightly delayed compared to that of heterozygous littermates (Fig. 5A, B). However, by E11.5-E11.75, Wnt4$^{-/-}$ lungs were distinctly smaller and displayed reduced branching, as compared to heterozygous littermates, in approximately 1/3 of the mutants (Fig. 5C, D). Both the left and right lung lobes were affected, however the reduction

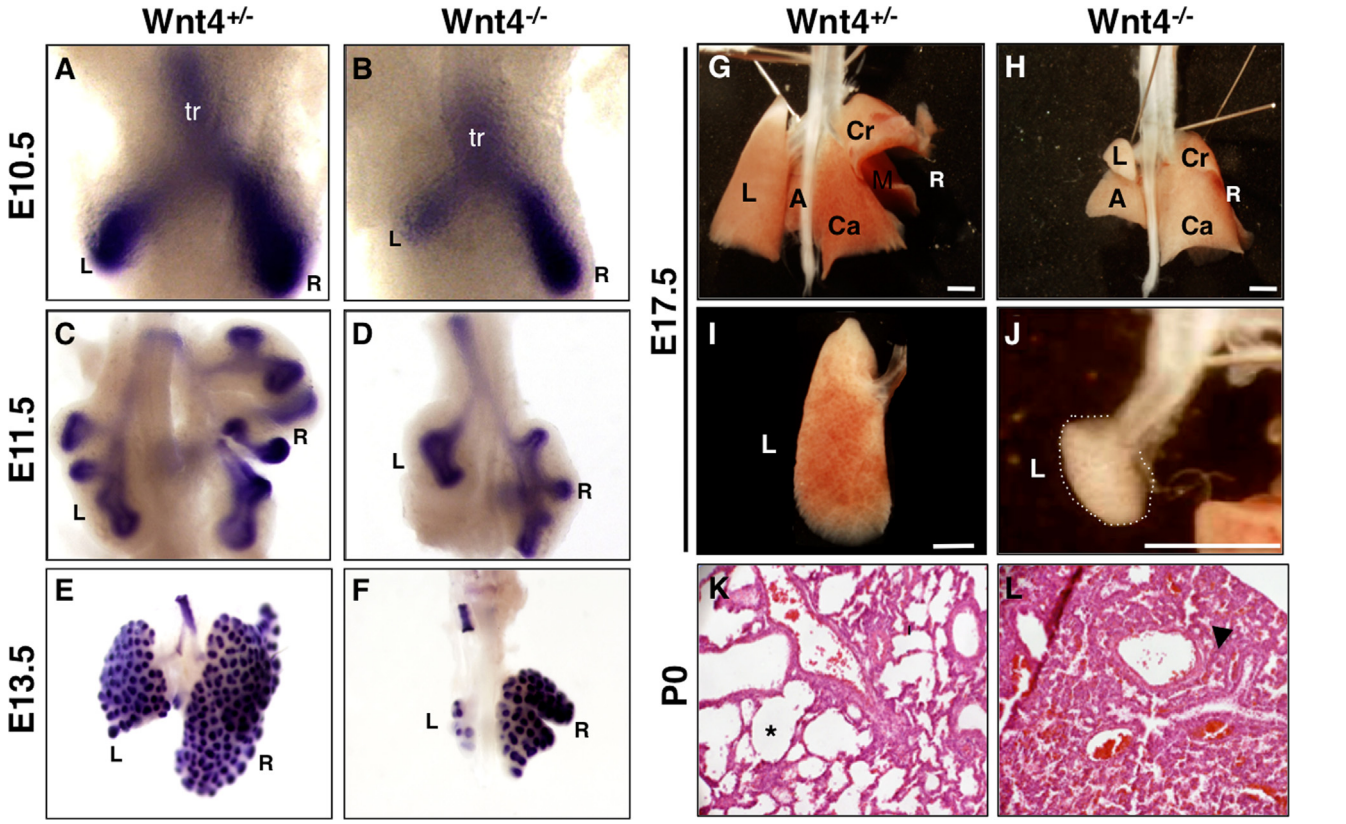

Fig. 5. Wnt4 null embryos display lung hypoplasia. (A)–(F) *In situ* hybridization for Wnt7b in Wnt4$^{+/-}$ (A), (C), and (E) or Wnt4$^{-/-}$ (B), (D), and (F) animals at E10.5 (A) and (B), E11.5 (C) and (D) or E13.5 (E) and (F). (G)–(J) Whole mount dorsal view of lungs from E17.5 Wnt4$^{+/-}$ (G) and (I) or Wnt4$^{-/-}$ (H) and (J) animals (left lung on left, L, and right lung on right, R). In (H), note severely reduced left lung bud (dotted line) compared to (G). Scale bar = 100 μM in (G)–(J). (K) and (L) H&E stained sections through P0 lungs from Wnt4$^{+/-}$ (K) or Wnt4$^{-/-}$ (L) littermates. Wnt4$^{-/-}$ lungs have dense cellularity, narrow or absent inflated air spaces (asterisk) and thicker intervalveolar septae (arrowhead). Lung bud lobes are labeled; A, accessory; Cr, cranial; Ca, caudal: L, left; R, right. tr, trachea.

was generally more pronounced in the left lobe.

By E13.5, the overall size of the lungs was markedly reduced in Wnt4$^{-/-}$ embryos, with 33% of mutants showing the most dramatic reduction (Fig. 5E, F). Indeed, the lung phenotypes was variable, with some embryos presenting severely reduced lungs, while others were slightly reduced (Fig. S4A-C). This hypoplasia persisted throughout embryogenesis until birth, (Fig. 5G–J andFig. S4D, E). Interestingly, organization of the major lobes was not disrupted, as a single left lobe and four right lobes could always be identified. However, while both left and right lobes were smaller than heterozygous lungs, the right lungs showed a less severe phenotype with about an average 20% reduction. Of the four right lobes, the posterior, superior and inferior right lobes were present but smaller, while the medial lobe was consistently reduced in size. The left lobe average size showed a 35% reduction as compared to controls. In about 15% of the cases, however, the left lung lobe was highly atrophic or almost absent (Fig. 5I, J). The absence of saccular structures in Wnt4$^{-/-}$ lung tissue indicates these lungs did not inflate after birth and is likely the cause of the rapid lethality observed in these mice (Fig. 5K, L). Our observations suggest that Wnt4 plays a critical role in lung development.

3.7. Wnt4$^{-/-}$ lungs are smaller due to reduced proliferation, not increased cell death

Because lung buds were reduced in size in the absence of Wnt4, we asked whether cell cycle or survival was affected during early development. TUNEL staining revealed no difference in apoptosis between Wnt4$^{+/-}$and Wnt4$^{-/-}$ lung buds, suggesting that loss of Wnt4 does not result in smaller lung buds due to cell death (Fig. 6A, B). We then examined phospho-Histone-H3 (pHH3) staining to assess whether a reduction in proliferation, during the time when lung buds are rapidly expanding, might account for the lung hypoplasia. We found that indeed, at both E10.75 and E11.5 (Fig. 6D–H) cells within the left bud showed significantly less proliferative capacity. In the left lung bud of the Wnt4$^{-/-}$ embryo, proliferation was significantly reduced in the mesoderm, however endoderm proliferation was unchanged (Fig. 6I). Proliferation was also highly decreased in both the proximal (termed L1 by (Metzger et al., 2008) and distal lung bud tips in Wnt4$^{-/-}$ embryos (Fig. 6J).

3.8. Lung Fgf9, Wnt2 and Sox9 expression are reduced in the absence of Wnt4

To examine why lung buds were hypoplastic in the absence of Wnt4, we further investigated the mechanism underlying the role that Wnt4 plays in lung development. We found that expression of the earliest marker of lung specification, Ttf1, was absent in the Wnt4$^{-/-}$ embryos at E8.5 when compared to their Wnt4$^{+/-}$ littermates (Fig. S5), even though it was detectable at normal levels in Wnt4$^{-/-}$ lungs at later stages (Fig. S6O, P). Given that ablation of Ttf1 does not result in failure of lung specification (Kimura et al., 1999), we considered additional growth factors known to impact lung development.

Indeed, several factors have been shown to play critical roles for the communication between lung epithelium and mesenchyme, including Wnts, BMPs and Fgfs. Wnt7b is known to be required for the normal development of both epithelium and smooth muscle cells, but its expression was largely unaffected in the Wnt4 mutants (Fig. 5A–F and data not shown) (Cohen et al.,

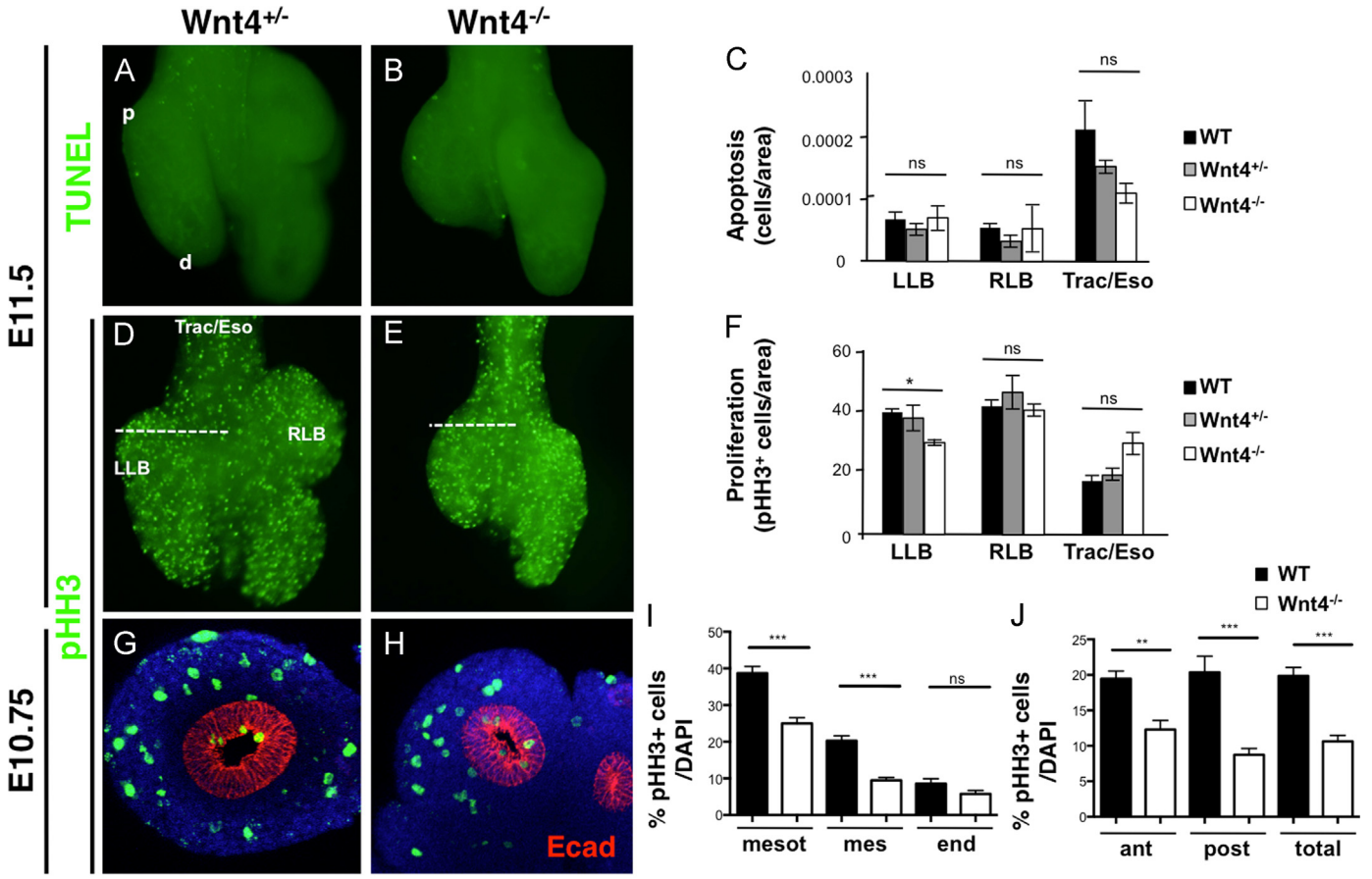

Fig. 6. Lung hypoplasia in Wnt4$^{-/-}$embryos results from decreased cell proliferation. TUNEL staining (A) and (B) or phospho-Histone-H3 (pHH3) immunofluorescence (D), (E), (G), and (H) of Wnt4$^{+/-}$ (A), (D), (G) or Wnt4$^{-/-}$ (B), (E), (H) lungs by wholemount staining at E11.5 (A), (B), (D), and (E) or on sections with E-cadherin (Ecad) immunofluorescence at E10.75 (G) and (H). (C) and (F) LLB, left lung bud; RLB, right lung bud. Buds extending at the proximal (p, also termed L1 in (Metzger et al., 2008) or distal (d) regions of either the LLB or RLB. (C) Quantification of TUNEL staining in E11.5 lung buds, $n=3$ (as in (A) and (B)). (F) Quantification of pHH3 staining in E11.5 whole mount lung buds, at location of nascent lung buds in anterior region of buds (dotted white line), $n=3$ (as in (D) and (E)). (I)–(J) Quantification of the ratio of pHH3^{+} cells over DAPI from E10.75 lung bud sections, $n=3$ (as in (G) and (H)). PHH3^{+} cells in endoderm (end, marked by Ecad), mesoderm (mes), and mesothelium (mesot) were quantified separately (I). Sections through the anterior (ant) and posterior (post) lung bud tips were also quantified separately (J). Data are shown as mean ± SEM; *$p<0.05$, **$p<0.01$, ***$p<0.001$, ns (not significant).

2009; Rajagopal et al., 2008). Similarly, numerous other candidate factors assessed by *in situ* hybridization at E13.5, including Bmp4, Bmp7, EfnB2, Shh and Wnt2b, all appeared grossly unchanged in expression at this later stage (Fig. S6).

We next examined Fgf10 and Fgf9, both secreted signaling essential to lung formation (Colvin et al., 2001; Sekine et al., 1999). Fgf10 and Fgf9 are expressed during early budding between E10.5 and E11.5, and are known to interact with the Wnt pathway to promote lung formation and branching. Fgf10 is normally expressed in the mesoderm at the tip of growing lung buds, in a dynamic and transient pattern. Fgf10 initiated relatively normally in both Wnt4$^{+/-}$ and Wnt4$^{-/-}$ embryonic lungs (Fig. S7A, B), but was slightly reduced throughout development in the lung bud tip mesoderm (Fig. S7C-H). Fgf10 reduction was confirmed by qPCR (Fig. S7I).

By contrast Fgf9 expression, which normally initiates in the mesothelium of the developing lung buds between E10.5 and 11.5 and is also expressed in the epithelium (Colvin et al., 1999; Colvin et al., 2001), was markedly reduced in the absence of Wnt4. In Wnt4$^{+/-}$ E11.5 embryos, Fgf9 was expressed at similar levels in both left and right lung buds (Fig. 7A, C). However, in Wnt4$^{-/-}$ embryos, we found that Fgf9 was significantly lower in the left lung bud compared to Wnt4$^{+/-}$ littermates when assayed by *in situ* hybridization (Fig. 7B, D). Given that Fgf9 has been suggested to regulate Wnt2 expression (Yin et al., 2011), we also examined Wnt2 expression in Wnt4$^{-/-}$ animals. Indeed we found a significant reduction in Wnt2 expression in the proximal lung bud that correlated with loss of Fgf9 expression (the location where new buds would emerge in the wildtype is indicated by black arrow, dotted line shows plane of section Fig. 7E, F). These findings were confirmed by qPCR analysis (Fig. S7I). Interestingly, and similar to our findings in the trachea, levels of Sox9 were also decreased in the absence of Wnt4 by qPCR. We propose that marked reduction in Fgf9, Wnt2 and Sox9 expression, and perhaps a more modest reduction in Fgf10, in the lungs of Wnt4 null mutants together result in reduced cell proliferation and lung hypoplasia (Fig. 8).

4. Discussion

In this study, we have identified a previously unknown site of Wnt4 expression within the mouse embryonic trunk and demonstrated that Wnt4 plays a critical role in the formation of the respiratory system. We find that Wnt4 is required for both tracheal and lung development. Specifically, Wnt4 is required for tracheal cartilage ring morphogenesis and for lung growth and branching. We find that in the lung, Wnt4 maintains appropriate levels of Fgf9, Wnt2 and Sox9, and is required for normal cell proliferation. These findings are of particular interest as multiple Wnts are

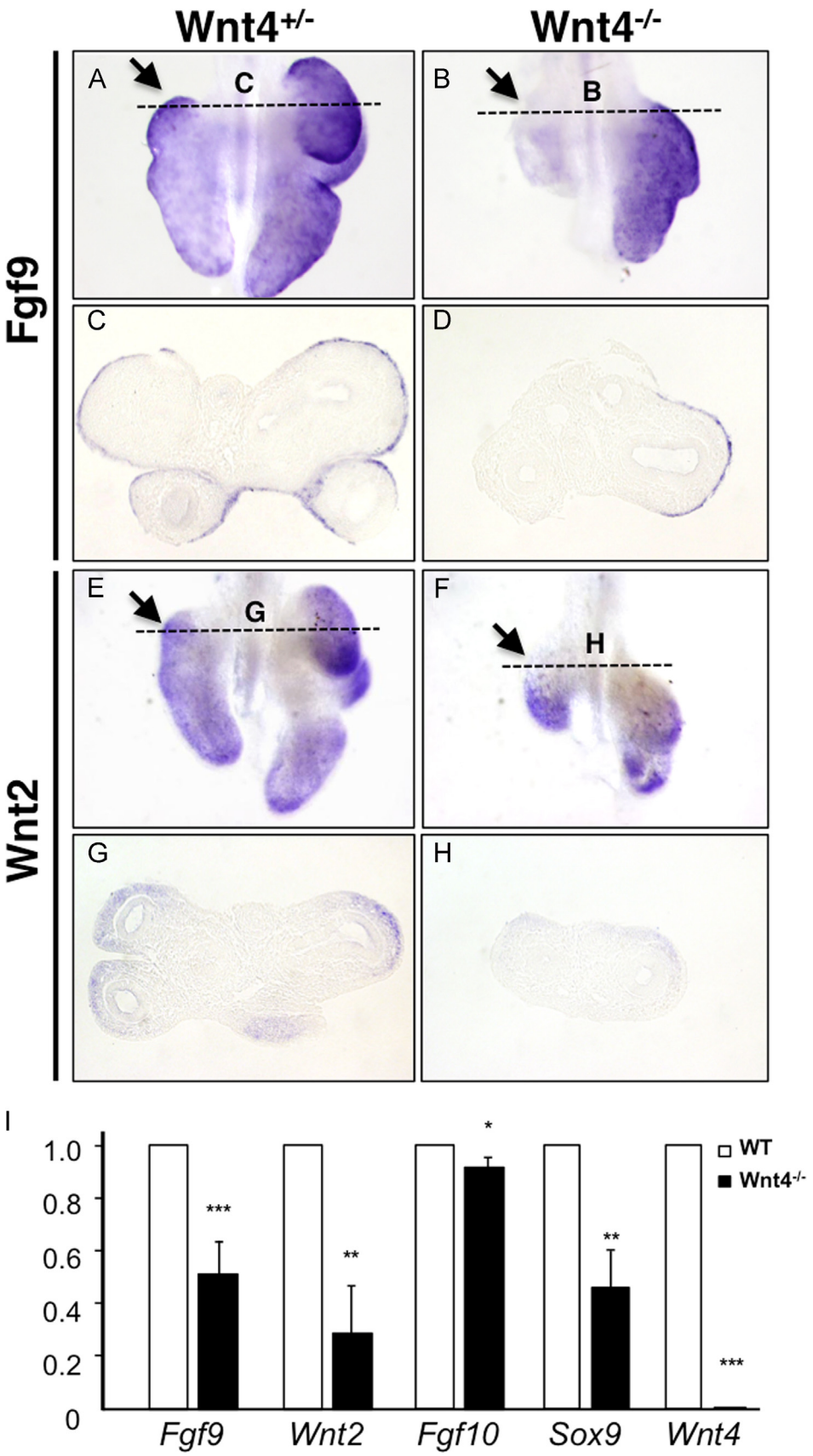

Fig. 7. Growth promoting Fgf9-Wnt2 signaling axis is reduced in Wnt4 deficient lung buds. Whole mount (A), (B), (E), and (F) or Section (C), (D), (G), and (H) *in situ* hybridization for Fgf9 (A)–(D) or Wnt2 (E)–(H) on $Wnt4^{+/-}$ (A), (C), (E), and (G) and $Wnt4^{-/-}$ (B), (D), (F), and (H) E11.75 lung buds. Note expression of both Fgf9 and Wnt2 are prominent in nascent lung buds (arrows) in Wnt4 heterozygotes. In the absence of Wnt4, both Fgf9 and Wnt2 expression are reduced in nascent lung buds, particularly in the left lobe and cranial part of the right lobe. Dotted line in (A), (B), (E), and (F) indicates the level of the sections shown in (C), (D), (G), and (H). (I) Quantification of *Fgf9*, *Wnt2* and *Fgf10* expression by qPCR analysis of E11.5 lung buds from WT and $Wnt4^{-/-}$ embryos. Data are shown as mean ± SEM; $^{*}p < 0.05$, $^{**}p < 0.01$, $^{***}p < 0.001$.

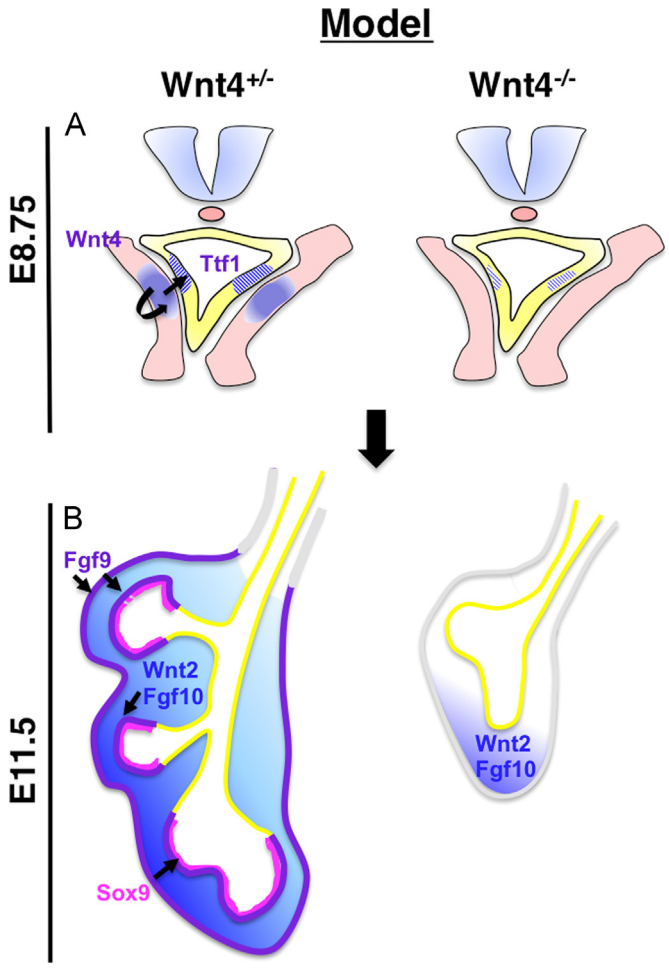

Fig. 8. Mesodermal Wnt4 helps initiate lung development and is required for proper levels of Fgf9, Wnt2 and Fgf10 in nascent lung buds. Schematic model showing: (A) requirement for Wnt4 in the splanchnic mesoderm for normal onset of lung specification in the absence of Wnt4; and (B) requirement for Wnt4 for high levels of mesenchymal Wnt2 and Fgf10 expression.

known to play critical roles during embryonic lung formation, however a role for Wnt4 had not previously been identified. These results place Wnt4 within a known network of Wnts, which coordinate to regulate development of the mammalian respiratory system, and further our understanding of the complex molecular underpinnings underlying lung development.

Wnt4 has been shown to be necessary for the development of the urinary and reproductive systems (Stark et al., 1994). Interestingly, however, it is known that absence of kidney results in death within 24–48 h after birth as a result of uremia, or the slow buildup of toxins in the blood. The fact that Wnt4 homozygous null mice die so rapidly after birth suggested that these mutants might have additional defects. Our analysis showed strong localized and transient Wnt4 expression near the presumptive respiratory territory that gives rise to the trachea, esophagus and lungs. While no defects were observed in some neighboring tissues (dorsal aorta or esophagus) in Wnt4$^{-/-}$ embryos, analysis of the trachea revealed abnormalities in its development. Defects were observed in the number of cartilage rings and fusion points. Among the genes shown to play a role in cartilage ring formation is Sox9 (Turcatel et al., 2013). Sox9 is involved in chondrocyte specification (Akiyama et al., 2002) and is known to interact with Wnt4 in the gonads (Chassot et al., 2012). We found Sox9 expression reduced in Wnt4 null mice, in both tracheal mesoderm and endoderm. Given that haploinsufficency or deletion of Sox9 both result in perinatal lethality due to bone and respiratory defects, including tracheal cartilage defects (Bi et al., 2001), we suggest reduced Sox9 levels in the Wnt null tracheas likely play a role in defects observed. Our findings identify Wnt4 as one of the factors required for normal tracheal ring formation.

The rapid postnatal lethality of the Wnt4 homozygous null mice was reminiscent of pups with defective lung formation, which die shortly after birth (Sekine et al., 1999). Indeed, the most striking phenotype in the Wnt4$^{-/-}$ embryonic trunk was the lung hypoplasia. Our study showed that Wnt4 expression is closely associated with the pre-lung domain between E8.75 and E9.5. In fact, Wnt4 in the mesoderm overlies a region of endoderm that expresses two important lung regulators: Wnt7b and Ttf1. Both Wnt7b and Ttf1 mark the lung epithelium and promote the proliferation of both epithelial and mesodermal lung cells in this region. Wnt4 precedes the expression of both Wnt7b and Ttf1 in the respiratory territory, suggesting it might induce their expression. However, Wnt7b is still expressed in the absence of Wnt4, and the onset of Ttf1 expression is only slightly delayed. These findings suggest that failure in lung development in Wnt4 null mice is not due to altered expression of these genes.

By contrast, Fgf9, Sox9 and Wnt2, all factors critical to lung development, are markedly reduced in Wnt4$^{-/-}$ lungs. Fgf9 is a secreted protein expressed in both the mesothelium and epithelium of the lungs, which has been shown to play a critical role in lung development. Ablation of Fgf9 has been shown to result in lung hypoplasia, due to both reduced branching and proliferation (Colvin et al., 2001). In Wnt4 null embryos, we observe lung hypoplasia by E10.5, two days earlier than that seen in Fgf9 null embryos. Interestingly, Fgf9 has been shown to be a direct target of β-catenin and therefore may be directly downstream of Wnt4 signaling (Karner et al., 2011; Park et al., 2012). Sox9 levels are also decreased in the absence of Wnt4 as revealed by qPCR. Loss of Sox9 is known to result in decreased proliferation and differentiation of the lung epithelium, however Sox9 has been shown not to be dependent on β-catenin activity (Rockich et al., 2013). Together, these findings suggest that the expression of select critical lung determinants depends on Wnt4, although likely not directly.

The more severe lung hypoplasia in Wnt4$^{-/-}$ embryos, when compared to Fgf9$^{-/-}$, may result from Wnt2, Sox9 and Fgf10 expression also being reduced in the absence of Wnt4. While lung Fgf10 expression initiates normally in the absence of Wnt4, its expression is detectably reduced in the lung mesenchyme between E11.5 and E13.5 (as shown by *in situ* hybridization and qPCR). Fgf10 is critical to lung outgrowth (Sekine et al., 1999; Weaver et al., 2000) and even a small reduction in Fgf10 signaling may impair lung development in the Wnt4 null embryos over time. It is possible that reduction in Fgf9 indirectly causes Fgf10 reduction. Fgf9 ablation was shown to impact Fgf10 expression, albeit only mildly (Colvin et al., 2001; Yin et al., 2011). Similarly, the impact of Wnt4 (and possibly Fgf9) reduction results in only a slight reduction of Fgf10 expression.

By contrast, loss of Wnt2 has been reported to result in significant hypoplasia of lung buds and double mutants for Wnt2 and Wnt2b show complete lung agenesis, suggesting they are required together for lung specification (Goss et al., 2009a). β-catenin, a key component of the canonical signaling pathway downstream of many Wnts, has been shown to be critical to both lung and trachea development (Harris-Johnson et al., 2009), further underlining the important role of Wnt signaling in this morphogenetic process. We find Wnt2 (but not Wnt2b) down-regulated in Wnt4 mutant lungs, particularly in the regions where new lung buds emerge (initiation of L1 bud). Given that Fgf9 and Wnt2 have been suggested to be the primary regulators involved in the maintenance of the mesenchymal Fgf-Wnt/β-catenin signaling driving lung

formation (Yin et al., 2011), we propose that Wnt4 influences initiation or proper strength of this signaling axis, and therefore results in more severe lung defects than in either of the single Fgf9$^{-/-}$ or Wnt2$^{-/-}$ embryos (Fig. 8).

Interestingly, we note that the impact of mesodermal Wnt4 on underlying endoderm must occur early during lung formation, as its expression is coincident with lung progenitor epithelium, but not with subsequent growing lung tissues. While at E8.75 Wnt4 mesodermal expression overlies endodermal epithelium expressing Ttf1, for instance, it shifts more dorsally as lung buds grow and extend ventrally. By E10.5, Wnt4 remains in the mesoderm of the future trachea (more dorsal), while lung epithelium expressing Ttf1 becomes restricted to the bronchial epithelium of the future lungs (more ventral). Given this progressive spatiotemporal separation of the lung from the trunk Wnt4 expression domain, we suggest that Wnt4 does not regulate later lung branching, but instead contributes an initiating signal required for subsequent outgrowth, via its impact on proliferation of mesenchymal cells of the early lung bud.

The intriguing question of why the left lung is more dramatically affected than the right lung in Wnt4 null mutants remains open. While we observe that Fgf9 is most dramatically reduced in the left lung bud by E11.5, it is still unclear why there is a differential requirement for Wnt4 on one side. Many reports that identify defects on one side of the developing lung find that it is the right lung that is generally more severely impacted in mutants such as Shh or Gli2 null embryos (Chiang et al., 1996; Mo et al., 1997). Future studies examining why and how the lung buds establish their left–right distinctive morphological features will be of great interest.

Also compelling is the observation that lesions in the Wnt4 gene have been linked to human disease. Wnt4 is known to be important during the development of the urinary and reproductive systems in humans (Biason-Lauber et al., 2004; Philibert et al., 2011). Interestingly, lesions in the Wnt4 gene have also been linked to pulmonary diseases, including chronic obstructive pulmonary disease (COPD) (Durham et al., 2013). In addition, one study shows that loss of Wnt4 function during human embryonic development results in SERKAL syndrome, which is characterized by female-to-male sex reversal, as well as renal, adrenal and lung hypoplasia (Mandel et al., 2008). This study correlates the absence of Wnt4 with lung hypoplasia in humans, thereby identifying a pivotal role for Wnt4 in the development of the respiratory system. Our study examining lung development in a mouse model of Wnt4 ablation confirms this role in both lung and trachea, and further examines the cellular and molecular mechanisms affected in the absence of this key regulator.

Acknowledgments

We are grateful to the MacDonald, Olson, Carroll and Cleaver labs for invaluable discussions and assistance, as well as Deneen Wellik for critical reading of the manuscript. We thank Peter Fletcher for his skilled (and cheerful) technical support. We also thank Jose Cabrera for his excellent artwork. This work was supported by NIH3R01DK079862 and 5F31DK092098 to LMS, and NIH R01 Grant DK079862-01 to OC.

Appendix A. Supplementary Information

Supplementary data associated with this article can be found in the online version at http://dx.doi.org/10.1016/j.ydbio.2015.08.017.

References

Akiyama, H., Chaboissier, M.C., Martin, J.F., Schedl, A., de Crombrugghe, B., 2002. The transcription factor Sox9 has essential roles in successive steps of the chondrocyte differentiation pathway and is required for expression of Sox5 and Sox6. Genes Dev. 16, 2813–2828.

Al Alam, D., Green, M., Tabatabai Irani, R., Parsa, S., Danopoulos, S., Sala, F.G., Branch, J., El Agha, E., Tiozzo, C., Voswinckel, R., Jesudason, E.C., Warburton, D., Bellusci, S., 2011. Contrasting expression of canonical Wnt signaling reporters TOPGAL, BATGAL and Axin2(LacZ) during murine lung development and repair. PLoS One 6, e23139.

Bi, W., Huang, W., Whitworth, D.J., Deng, J.M., Zhang, Z., Behringer, R.R., de Crombrugghe, B., 2001. Haploinsufficiency of Sox9 results in defective cartilage primordia and premature skeletal mineralization. Proc. Natl. Acad. Sci. USA 98, 6698–6703.

Biason-Lauber, A., Konrad, D., Navratil, F., Schoenle, E.J., 2004. A WNT4 mutation associated with Mullerian-duct regression and virilization in a 46,XX woman. N. Engl. J. Med. 351, 792–798.

Brisken, C., Heineman, A., Chavarria, T., Elenbaas, B., Tan, J., Dey, S.K., McMahon, J.A., McMahon, A.P., Weinberg, R.A., 2000. Essential function of Wnt-4 in mammary gland development downstream of progesterone signaling. Genes Dev. 14, 650–654.

Carroll, S.F., Buckley, C.T., Kelly, D.J., 2014. Cyclic hydrostatic pressure promotes a stable cartilage phenotype and enhances the functional development of cartilaginous grafts engineered using multipotent stromal cells isolated from bone marrow and infrapatellar fat pad. J. Biomech. 47, 2115–2121.

Chassot, A.A., Bradford, S.T., Auguste, A., Gregoire, E.P., Pailhoux, E., de Rooij, D.G., Schedl, A., Chaboissier, M.C., 2012. WNT4 and RSPO1 together are required for cell proliferation in the early mouse gonad. Development 139, 4461–4472.

Chiang, C., Litingtung, Y., Lee, E., Young, K.E., Corden, J.L., Westphal, H., Beachy, P.A., 1996. Cyclopia and defective axial patterning in mice lacking Sonic hedgehog gene function. Nature 383, 407–413.

Chong, D.C., Koo, Y., Xu, K., Fu, S., Cleaver, O., 2011. Stepwise arteriovenous fate acquisition during mammalian vasculogenesis. Dev. Dyn. 240, 2153–2165.

Cohen, E.D., Ihida-Stansbury, K., Lu, M.M., Panettieri, R.A., Jones, P.L., Morrisey, E.E., 2009. Wnt signaling regulates smooth muscle precursor development in the mouse lung via a tenascin C/PDGFR pathway. J. Clin. Investig. 119, 2538–2549.

Colvin, J.S., Feldman, B., Nadeau, J.H., Goldfarb, M., Ornitz, D.M., 1999. Genomic organization and embryonic expression of the mouse fibroblast growth factor 9 gene. Dev. Dyn. 216, 72–88.

Colvin, J.S., White, A.C., Pratt, S.J., Ornitz, D.M., 2001. Lung hypoplasia and neonatal death in Fgf9-null mice identify this gene as an essential regulator of lung mesenchyme. Development 128, 2095–2106.

Das, A., Tanigawa, S., Karner, C.M., Xin, M., Lum, L., Chen, C., Olson, E.N., Perantoni, A.O., Carroll, T.J., 2013. Stromal-epithelial crosstalk regulates kidney progenitor cell differentiation. Nat. Cell Biol. 15, 1035–1044.

DasGupta, R., Fuchs, E., 1999. Multiple roles for activated LEF/TCF transcription complexes during hair follicle development and differentiation. Development 126, 4557–4568.

Dean, C.H., Miller, L.A., Smith, A.N., Dufort, D., Lang, R.A., Niswander, L.A., 2005. Canonical Wnt signaling negatively regulates branching morphogenesis of the lung and lacrimal gland. Dev. Biol. 286, 270–286.

Durham, A.L., McLaren, A., Hayes, B.P., Caramori, G., Clayton, C.L., Barnes, P.J., Chung, K.F., Adcock, I.M., 2013. Regulation of Wnt4 in chronic obstructive pulmonary disease. FASEB J. 27, 2367–2381.

Gordon, M.D., Nusse, R., 2006. Wnt signaling: multiple pathways, multiple receptors, and multiple transcription factors. J. Biol. Chem. 281, 22429–22433.

Goss, A.M., Tian, Y., Tsukiyama, T., Cohen, E.D., Zhou, D., Lu, M.M., Yamaguchi, T.P., Morrisey, E.E., 2009a. Wnt2/2b and beta-catenin signaling are necessary and sufficient to specify lung progenitors in the foregut. Dev. Cell 17, 290–298.

Goss, A.M., Tian, Y., Tsukiyama, T., Cohen, E.D., Zhou, D., Lu, M.M., Yamaguchi, T.P., Morrisey, E.E., 2009b. Wnt2/2b and beta-catenin signaling are necessary and sufficient to specify lung progenitors in the foregut. Dev. Cell 17, 290–298.

Grigoryan, T., Wend, P., Klaus, A., Birchmeier, W., 2008. Deciphering the function of canonical Wnt signals in development and disease: conditional loss- and gain-of-function mutations of beta-catenin in mice. Genes Dev. 22, 2308–2341.

Harris-Johnson, K.S., Domyan, E.T., Vezina, C.M., Sun, X., 2009. Beta-catenin promotes respiratory progenitor identity in mouse foregut. Proc. Natl. Acad. Sci. USA 106, 16287–16292.

Heikkila, M., Peltoketo, H., Leppaluoto, J., Ilves, M., Vuolteenaho, O., Vainio, S., 2002. Wnt-4 deficiency alters mouse adrenal cortex function, reducing aldosterone production. Endocrinology 143, 4358–4365.

Heinonen, K.M., Vanegas, J.R., Brochu, S., Shan, J., Vainio, S.J., Perreault, C., 2011. Wnt4 regulates thymic cellularity through the expansion of thymic epithelial cells and early thymic progenitors. Blood 118, 5163–5173.

Kadzik, R.S., Cohen, E.D., Morley, M.P., Stewart, K.M., Lu, M.M., Morrisey, E.E., 2014. Wnt ligand/Frizzled 2 receptor signaling regulates tube shape and branch-point formation in the lung through control of epithelial cell shape. Proc. Natl. Acad. Sci. USA 111, 12444–12449.

Karner, C.M., Das, A., Ma, Z., Self, M., Chen, C., Lum, L., Oliver, G., Carroll, T.J., 2011. Canonical Wnt9b signaling balances progenitor cell expansion and differentiation during kidney development. Development 138, 1247–1257.

Kaufman, M.H., 1992. Atlas of Mouse Development. Elsevier Academic Press, San Diego, CA USA, Revised Edition ed.

Kim, B.M., Buchner, G., Miletich, I., Sharpe, P.T., Shivdasani, R.A., 2005. The stomach

mesenchymal transcription factor Barx1 specifies gastric epithelial identity through inhibition of transient Wnt signaling. Dev. Cell 8, 611–622.
Kim, Y., Kobayashi, A., Sekido, R., DiNapoli, L., Brennan, J., Chaboissier, M.C., Poulat, F., Behringer, R.R., Lovell-Badge, R., Capel, B., 2006. Fgf9 and Wnt4 act as antagonistic signals to regulate mammalian sex determination. PLoS Biol. 4, e187.
Kimura, S., Ward, J.M., Minoo, P., 1999. Thyroid-specific enhancer-binding protein/thyroid transcription factor 1 is not required for the initial specification of the thyroid and lung primordia. Biochimie 81, 321–327.
Konigshoff, M., Eickelberg, O., 2010. WNT signaling in lung disease: a failure or a regeneration signal? Am. J. Respir. Cell Mol. Biol. 42, 21–31.
Krausova, M., Korinek, V., 2014. Wnt signaling in adult intestinal stem cells and cancer. Cell. Signal. 26, 570–579.
Li, C., Xiao, J., Hormi, K., Borok, Z., Minoo, P., 2002. Wnt5a participates in distal lung morphogenesis. Dev. Biol. 248, 68–81.
Mandel, H., Shemer, R., Borochowitz, Z.U., Okopnik, M., Knopf, C., Indelman, M., Drugan, A., Tiosano, D., Gershoni-Baruch, R., Choder, M., Sprecher, E., 2008. SERKAL syndrome: an autosomal-recessive disorder caused by a loss-of-function mutation in WNT4. Am. J. Hum. Genet. 82, 39–47.
Metzger, R.J., Klein, O.D., Martin, G.R., Krasnow, M.A., 2008. The branching programme of mouse lung development. Nature 453, 745–750.
Mo, R., Freer, A.M., Zinyk, D.L., Crackower, M.A., Michaud, J., Heng, H.H., Chik, K.W., Shi, X.M., Tsui, L.C., Cheng, S.H., Joyner, A.L., Hui, C., 1997. Specific and redundant functions of Gli2 and Gli3 zinc finger genes in skeletal patterning and development. Development 124, 113–123.
Molin, D.G., DeRuiter, M.C., Wisse, L.J., Azhar, M., Doetschman, T., Poelmann, R.E., Gittenberger-de Groot, A.C., 2002. Altered apoptosis pattern during pharyngeal arch artery remodelling is associated with aortic arch malformations in Tgfbeta2 knock-out mice. Cardiovasc. Res. 56, 312–322.
Moore, K.L., Persaud, T.V.N., 1993. The Cardiovascular System. The Developing Human. Clinically Oriented Embryology. W.B. Saunders, Co., pp. 304–353.
Morrisey, E.E., Hogan, B.L., 2010. Preparing for the first breath: genetic and cellular mechanisms in lung development. Dev. Cell 18, 8–23.
Naylor, R.W., Jones, E.A., 2009. Notch activates Wnt-4 signalling to control mediolateral patterning of the pronephros. Development 136, 3585–3595.
Nusse, R., Varmus, H.E., 1982. Many tumors induced by the mouse mammary tumor virus contain a provirus integrated in the same region of the host genome. Cell 31, 99–109.
Park, J.S., Ma, W., O'Brien, L.L., Chung, E., Guo, J.J., Cheng, J.G., Valerius, M.T., McMahon, J.A., Wong, W.H., McMahon, A.P., 2012. Six2 and Wnt regulate self-renewal and commitment of nephron progenitors through shared gene regulatory networks. Dev. Cell 23, 637–651.
Philibert, P., Biason-Lauber, A., Gueorguieva, I., Stuckens, C., Pienkowski, C., Lebon-Labich, B., Paris, F., Sultan, C., 2011. Molecular analysis of WNT4 gene in four adolescent girls with mullerian duct abnormality and hyperandrogenism (atypical Mayer–Rokitansky–Kuster–Hauser syndrome). Fertil. Steril. 95, 2683–2686.
Pinto, D., Gregorieff, A., Begthel, H., Clevers, H., 2003. Canonical Wnt signals are essential for homeostasis of the intestinal epithelium. Genes Dev. 17, 1709–1713.
Rajagopal, J., Carroll, T.J., Guseh, J.S., Bores, S.A., Blank, L.J., Anderson, W.J., Yu, J., Zhou, Q., McMahon, A.P., Melton, D.A., 2008. Wnt7b stimulates embryonic lung growth by coordinately increasing the replication of epithelium and mesenchyme. Development 135, 1625–1634.
Rockich, B.E., Hrycaj, S.M., Shih, H.P., Nagy, M.S., Ferguson, M.A., Kopp, J.L., Sander, M., Wellik, D.M., Spence, J.R., 2013. Sox9 plays multiple roles in the lung epithelium during branching morphogenesis. Proc. Natl. Acad. Sci. USA 110, E4456–E4464.
Saulnier, D.M., Ghanbari, H., Brandli, A.W., 2002. Essential function of Wnt-4 for tubulogenesis in the *Xenopus pronephric* kidney. Dev. Biol. 248, 13–28.
Segre, J.A., Bauer, C., Fuchs, E., 1999. Klf4 is a transcription factor required for establishing the barrier function of the skin. Nat. Genet. 22, 356–360.
Sekine, K., Ohuchi, H., Fujiwara, M., Yamasaki, M., Yoshizawa, T., Sato, T., Yagishita, N., Matsui, D., Koga, Y., Itoh, N., Kato, S., 1999. Fgf10 is essential for limb and lung formation. Nat. Genet. 21, 138–141.
Shu, W., Jiang, Y.Q., Lu, M.M., Morrisey, E.E., 2002. Wnt7b regulates mesenchymal proliferation and vascular development in the lung. Development 129, 4831–4842.
Stark, K., Vainio, S., Vassileva, G., McMahon, A.P., 1994. Epithelial transformation of metanephric mesenchyme in the developing kidney regulated by Wnt-4. Nature 372, 679–683.
Strochlic, L., Falk, J., Goillot, E., Sigoillot, S., Bourgeois, F., Delers, P., Rouviere, J., Swain, A., Castellani, V., Schaeffer, L., Legay, C., 2012. Wnt4 participates in the formation of vertebrate neuromuscular junction. PLoS One 7, e29976.
Thomas, K.R., Capecchi, M.R., 1990. Targeted disruption of the murine int-1 proto-oncogene resulting in severe abnormalities in midbrain and cerebellar development. Nature 346, 847–850.
Treier, M., Gleiberman, A.S., O'Connell, S.M., Szeto, D.P., McMahon, J.A., McMahon, A.P., Rosenfeld, M.G., 1998. Multistep signaling requirements for pituitary organogenesis in vivo. Genes Dev. 12, 1691–1704.
Turcatel, G., Rubin, N., Menke, D.B., Martin, G., Shi, W., Warburton, D., 2013. Lung mesenchymal expression of Sox9 plays a critical role in tracheal development. BMC Biol. 11, 117.
Vainio, S., Heikkila, M., Kispert, A., Chin, N., McMahon, A.P., 1999. Female development in mammals is regulated by Wnt-4 signalling. Nature 397, 405–409.
Weaver, M., Dunn, N.R., Hogan, B.L., 2000. Bmp4 and Fgf10 play opposing roles during lung bud morphogenesis. Development 127, 2695–2704.
Yin, Y., Wang, F., Ornitz, D.M., 2011. Mesothelial- and epithelial-derived FGF9 have distinct functions in the regulation of lung development. Development 138, 3169–3177.